

RESIDUAL-GAS-IONIZATION BEAM PROFILE MONITORS IN RHIC*

R. Connolly, R. Michnoff, and S. Tepikian
 Brookhaven National Lab, Upton, NY, USA

Abstract

Four ionization profile monitors (IPMs) in RHIC measure vertical and horizontal beam profiles in the two rings by measuring the distribution of electrons produced by beam ionization of residual gas. During the last three years both the collection accuracy and signal/noise ratio have been improved. An electron source is mounted across the beam pipe from the collector to monitor microchannel plate (MCP) aging and the signal electrons are gated to reduce MCP aging and to allow charge replenishment between single-turn measurements. Software upgrades permit simultaneous measurements of any number of individual bunches in the ring. This has been used to measure emittance growth rates on six bunches of varying intensities in a single store. Also the software supports FFT analysis of turn-by-turn profiles of a single bunch at injection to detect dipole and quadrupole oscillations.

INTRODUCTION

The Relativistic Heavy Ion Collider (RHIC) at Brookhaven National Lab [1] has four ionization profile monitors (IPMs) [2,3,4] for measuring the horizontal and vertical beam profiles in each of the two rings. An IPM measures the transverse beam profile by collecting and measuring the distribution of electrons generated by ionization of residual gas in the beamline. Similar detectors are used at Fermi National Lab [5], DESY [6], and CERN [7].

Since 1999 the detectors have been upgraded during each machine shutdown to reduce problems that arose in the previous run. As the measurement capability has improved features have been added to the application software based on the requests of the accelerator physicists.

In the next section we describe the design and performance of the detector. Then there is a section describing the software. We then give several examples of beam measurements during the 2005 copper and proton runs where the IPMs contributed significantly to understanding the machine operation. Finally there is a discussion of outstanding issues and plans for the future.

DETECTOR

An IPM works by sweeping electrons produced by beam ionization of background gas to the side of the beam pipe and measuring their distribution transverse to the beam. Figure 1 is a schematic of the detector and its

associated electronics in the accelerator tunnel. The detector chamber is located in a section of 10x15cm rectangular pipe. In an 18-cm-long section of this beam pipe half of the pipe has been removed and a saddle piece inserted. This saddle piece is biased at -8kV producing an accurate transverse electric field of 10^5 V/m.

A rectangular opening in the grounded half of the beam pipe allows the signal electrons to strike a 8x10cm microchannel plate [8]. This opening is covered by an hexagonal aluminum mesh from Laird [9] which has 95% open area and attenuates rf by 100dB. This places the electronics out of the path of the image current and presents a continuous beamline cross section to the beam. Also the MCP is in an alcove which shields it from radiation spray from upstream beam loss. A dipole magnetic field of 0.12T forces the electrons to travel perpendicular to the collection plane.

The amplified electron flux is collected on an anode board with 64 channels. Each channel is connected via vacuum feedthrough to a preamplifier which drives a shielded twisted-pair transmission line to a 10MSPS VME digitizer.

For the 2005 run a signal-gating grid was added inside the beampipe. Each channel of an MCP has a dead time of about 1ms after firing. The intense heavy-ion beams of RHIC create such a large signal flux that the plate gain in the center of the beam was dynamically suppressed. Also an MCP can deliver a lifetime charge of approximately 0.1-1.0C/cm². Without signal gating the MCPs failed before the end of the 2004 run. For a routine measurement the grid is pulled to ground by a Behlke [10] transistor switch for a full turn. During this turn the digitizers are triggered. The grid is then returned to the sweep voltage for 100 turns. This is repeated 100 times and the data are averaged.

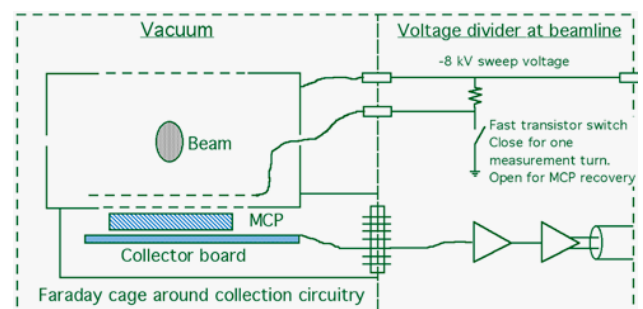


Figure 1: Schematic of detector and electronics located at the beamline.

*Work performed under the auspices of the United States Department of Energy

MEASUREMENT CAPABILITY

The two data collection modes are shown in the timing diagram, fig. 2. In the normal mode the signal gate is opened for one full turn and the digitizers are triggered on the selected rf buckets. The IPM is fast enough to resolve individual bunches. After one turn both trigger signals are off for 99 turns to allow charge replenishment in the MCPs. The two trigger signals are generated by two channels of the V124 VME timing module [11].

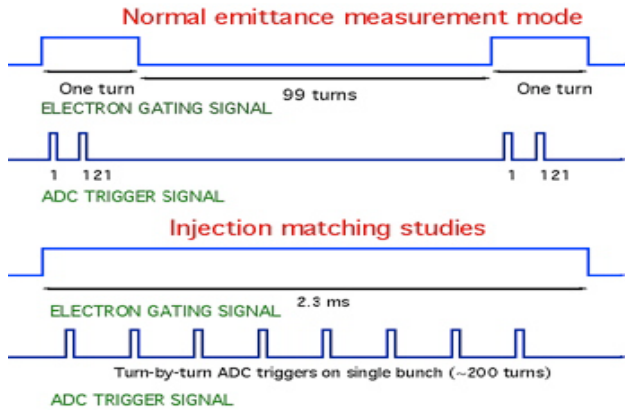


Figure 2: Data collection timing diagrams showing the normal profile measurement mode (top) and the special injection-matching mode.

An example of multiple bunch measurements is shown in fig. 3. These data were taken during measurements of emittance growth from intra-beam scattering [12]. Here six rf buckets are populated with different bunch sizes and emittance is monitored for one hour. In this case multiple-bunch acquisition allows simultaneous multiple measurements.

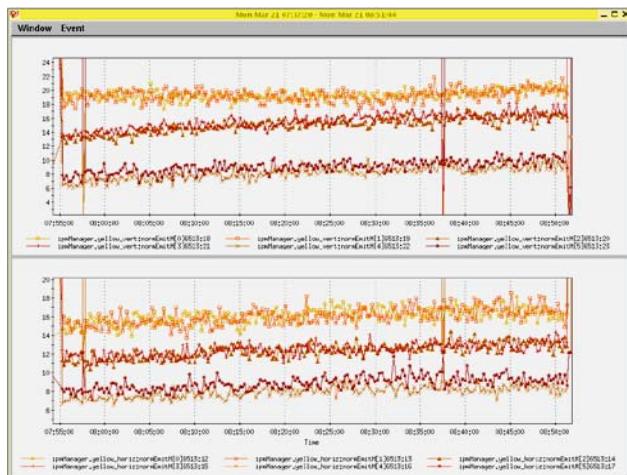


Figure 3. Simultaneous emittance measurements on six bunches of different intensities. Measurements period is one hour.

For injection studies with heavy-ion beams the IPMs can be operated in single-turn mode. The signal gate is left on for 128 turns and a single bunch is measured on consecutive turns. For each profile the center and width of the profile is calculated and FFTs are made from these records to detect betatron and quadrupole oscillations.

Figure 4 shows the power spectrum page from the application. This example shows coupling between planes by monitoring a bunch injected at an angle with the Yellow vertical IPM. In one plane the amplitude is beating at the difference between the horizontal and vertical tunes (top). The dipole spectrum shows the two betatron frequencies (second plot). There is no quadrupole oscillation.

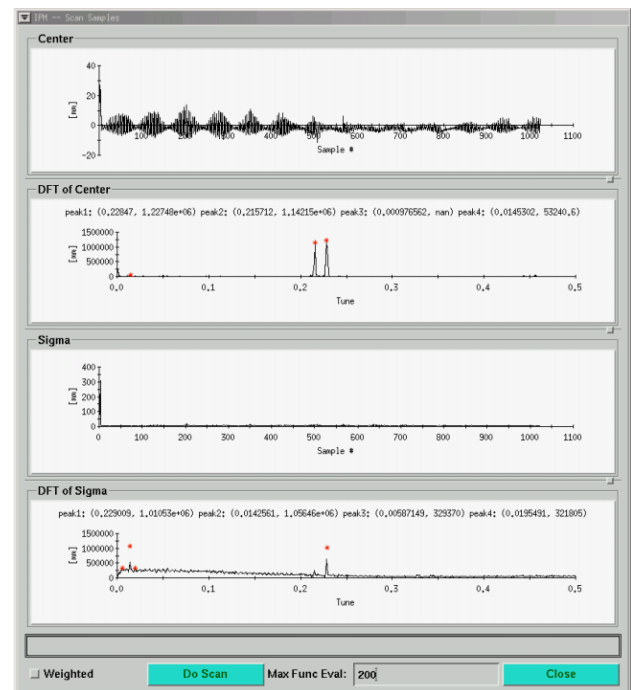


Figure 4. Power spectrum page from the application. The beam was injected at an angle producing betatron oscillations. The amplitude in this plane is beating at the difference between the vertical and horizontal tunes (top). The two tunes are shown in the second plot.

BEAM MEASUREMENTS

During the 2005 copper [13] and proton RHIC runs the IPMs were widely used in diagnosing machine problems and in machine physics studies. In this section we give several examples together with references to papers that analyze IPM data. This section is not intended to be a complete listing of IPM measurements.

Instability at transition

During the 2005 Cu run the beam in the yellow ring experienced an instability at transition which resulted in beam loss. This is believed to be a single-bunch instability triggered by tune shift caused by electron cloud buildup [14]. Figure 5 shows the yellow-ring IPM records of this instability. Six bunches are being monitored. Before transition all six bunches have the same emittance. After transition the bunches in buckets 19 and 61 are undisturbed and buckets 1, 100, 109 and 121 experience emittance blowup. Buckets 100 and 121 are almost empty. This instability was avoided by limiting beam intensity and adjusting chromaticity.

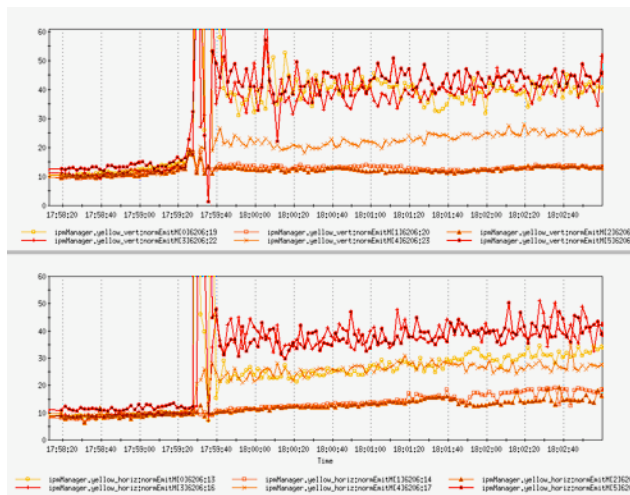


Figure 5. Emittance measurements on six bunches during an instability ramp. Four of six bunches blow up at transition. The top is vertical and bottom horizontal.

IBS measurements

Intra-beam scattering is a leading mechanism of emittance growth in heavy-ion storage rings [12]. The IPM is the instrument that has been used to measure transverse emittance growth in RHIC. By taking advantage of its multiple-bunch measuring capability it is possible to measure simultaneously growth rates on several bunches of different intensities. This saves time since the growth typically is monitored for an hour and it also ensures that the bunch intensity is the only parameter varied in the experiment.

Figure 6, reproduced from ref. 12, shows the measured growth rates of two bunches compared with the results from computer models. These data were taken on two Cu bunches of 6×10^8 (top) and 3×10^8 ions/bunch.

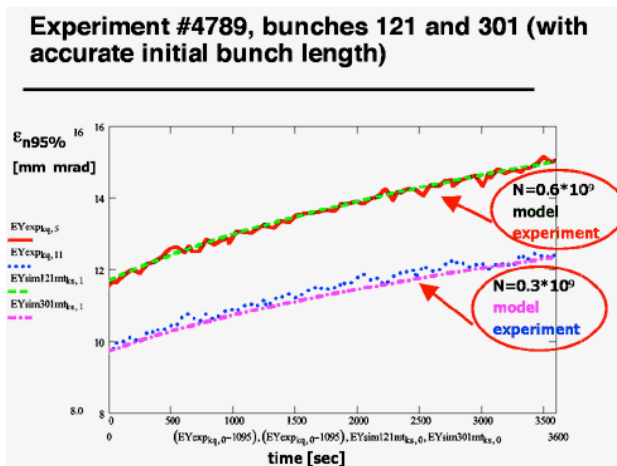


Figure 6. Plots showing emittance growth measurements compared to predicted rates from model. These data were taken over one hour on two bunches.

Abort-gap cleaning and beam-beam effects

As emittance grows during a store the beam gradually debunches and coasting beam accumulates [15]. The coasting beam causes a significant increase in experimental backgrounds. Eventually the coasting beam has to be removed and the abort gap cleaned. This was done by firing the tune kickers in the abort gap several times in each store. However the cleaning process caused a large increase in experimental backgrounds so the detectors were turned off during the process. This method reduced the integrated luminosity over a store by $\sim 20\%$.

Early in the 2005 run continuous gap cleaning was tried by firing the tune kicker about once a minute. Figure 7 shows six-bunch IPM data taken in the yellow ring during gap cleaning studies. In this figure the top graph is the vertical IPM and the bottom is horizontal. It was found that ringing in the kicker affected the bunch in bucket 1 (top trace) but none of the other bunches. Since the coasting beam is continuously removed it does not build up to the point the detectors have to be turned off during the store, significantly increasing integrated luminosity.

Also on fig. 7 are growth records from four other bunches. The three grouped together are in buckets 19, 37 and 121. These bunches experienced four collisions/turn. The bottom trace is the bunch in bucket 100, a three-collision bunch. These data indicate that emittance growth is higher in the four-collision bunches than the three-collision bunch. This is strong indication of beam-beam emittance growth. The bunch in bucket 61, the one kicked for tune measurements, is off this graph.

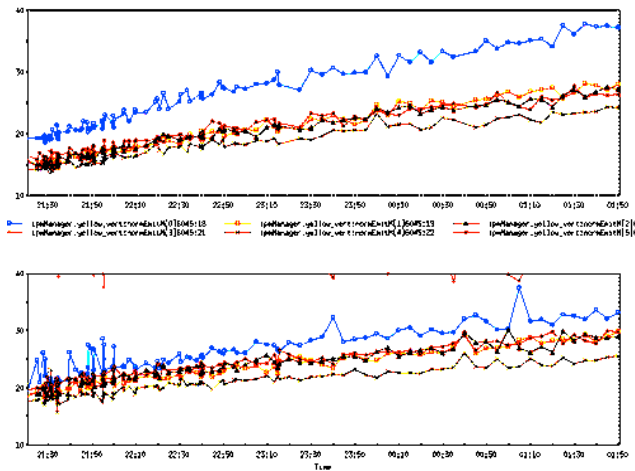


Figure 7. A five-hour record of six bunches in the yellow ring with vertical on top and horizontal on bottom. The top trace is bucket 1 which is kicked during gap cleaning.

Dynamic aperture

The dynamic apertures of RHIC are measured by kicking a bunch with the tune kicker and monitoring the emittance of that bunch with the IPM and the bunch intensity with the wall current monitor. An example of a measurement made during the 2004 run is shown in fig. 8. The top plot is the bunch intensity and the bottom is the normalized emittance. Several bunches were injected into RHIC and each was kicked with the tune kicker until the wall-current monitor showed loss from the kicked bunch.

The figure shows the results from three different lattice conditions. The three lattices give dynamic emittance apertures of 210, 260 and $100 \times 10^{-6} \text{m}$. This measurement showed that the predetermined settings of the strong interaction region octupoles severely restricted the dynamic aperture and this problem was then fixed. As the time axis shows, the single bunch capability of the IPM permitted three measurements to be made in slightly more than one hour.

Polarimeter measurements

The proton-beam polarimeter is based on proton carbon elastic scattering in the Coulomb Nuclear Interference region [16]. A $400 \mu\text{m}$ carbon ribbon is inserted into the beam for about two minutes for each measurement. Figure 9 shows beam profiles before (top) and after a polarization measurement. From left to right there are blue horizontal and vertical and yellow horizontal and vertical profiles. The blue beam shows no emittance growth and the yellow shows about 50% growth. When this was investigated it was found that the yellow polarimeter gave twice the signal as in blue indicating the yellow target was larger.

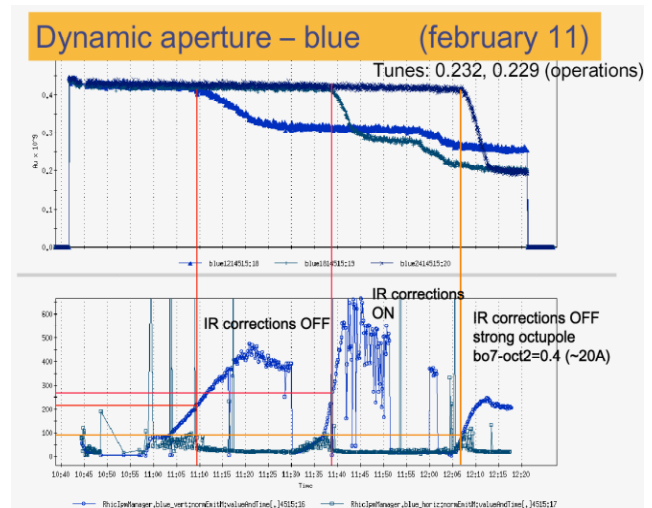


Figure 8. Dynamic aperture studies in RHIC with AU beam. Three bunches were kicked and the intensity (top) and emittance were measured. The dynamic aperture is the emittance where beam loss begins.

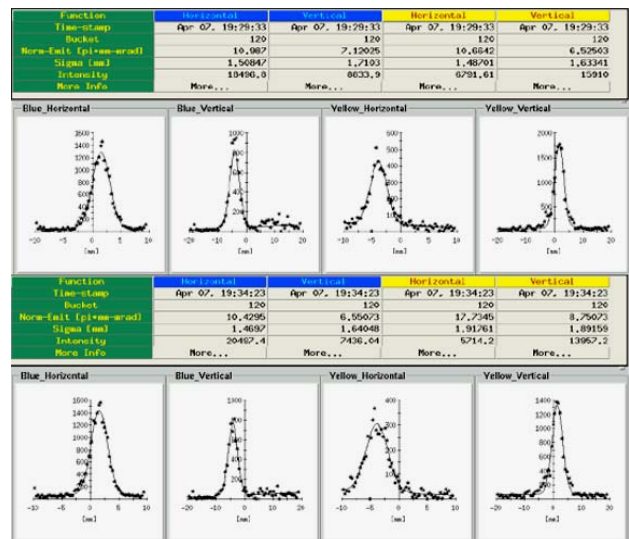


Figure 9. Beam profiles before (top) and after a polarization measurement. The carbon ribbon in yellow was wider than in blue resulting in yellow emittance growth.

DISCUSSION

The RHIC IPMs have been continually improved over the past five beam runs. Problems which have been largely solved are rf coupling to the beam, dynamic gain reduction of the MCPs from high signal fluxes, background from radiation spray, background from electron cloud buildup, and permanent MCP damage from high integrated signal flux. The IPMs have performed reliably through the entire 2005 copper and proton runs.

The dynamic gain reduction and short MCP lifetimes were greatly improved for this run by the addition of the fast electron-signal gating. As is often the case however, the signal gating has introduced a couple of new problems which we hope to correct during the next shutdown period.

During this run we observed large backgrounds resulting from the beam-image current coupling into the collectors. This background is new and differs from previous noise problems in that from turn to turn the backgrounds on the IPM channels do not change. Because of this we were able to take data with the electron gate open and closed and subtract away the background. All data shown for the copper beam have this background subtraction.

Another challenge is to decouple the gating grid from the beam. For the copper beam the gating grid deflects the beam about 0.1 μ radians. For a typical measurement it is fired 100 times on every hundredth turn. This puts a driving source at about 780Hz. Transverse measurements made using beam position monitors as pickups show that the IPMs leave a coherent oscillation in the beam when the tune is on a harmonic of the gate switching frequency [17].

During the next RHIC shutdown one IPM will be placed on a test stand. We will try to reproduce the image current coupling via taut-wire measurements. If this coupling can be reproduced we will explore methods to reduce it. The capacitive coupling to the beam can be reduced by introducing a grounded grid between the gate and the beam but we are running out of room between the magnet pole tips. Another fix that is being explored is to vary the number of turns between gate firings during the measurement. This would spread the drive power over a wide range of frequencies instead of putting all power into one line.

The software is in place for single bunch turn-by-turn measurement for injection matching. However this will not become a routine measurement until the image current coupling is greatly reduced.

CONCLUSION

The RHIC IPMs have matured into useful and dependable beam emittance monitors. Electron collection in a magnetic field is accurate and fast enough to measure single heavy-ion bunches separated by 100ns. Multiple bunch measurements have been useful in diagnosing single-bunch instabilities and evaluating continuous gap cleaning. Also the multiple-bunch capability has been a great time saver during machine studies when multiple measurements can be made with a single machine fill.

ACKNOWLEDGEMENTS

During the last two RHIC shutdown periods major modifications have been made to the IPMs. Manuel Grau and Charles Trabocchi did most of the design and assembly work. Figures and ideas for examples have been contributed by Mei Bai, Vadim Ptitsyn, Alexei Fedotov, Angelika Drees, Fulvia Pilat, Jie Wei and Haixin Huang.

REFERENCES

- [1] <http://www.bnl.gov/RHIC>
- [2] R. Connolly, R. Michnoff, T. Moore, T. Shea, and S. Tepikian, Nucl. Instr. and Meth. A 443 (2000) 215-222.
- [3] Connolly, R., Cameron, P., Michnoff, R., and Tepikian, S., *Performance of the RHIC IPM*, Proc. 2001 PAC, Chicago.
- [4] R. Connolly, M. Grau, R. Michnoff and S. Tepikian, "The IPM as a Halo Measurement and Prevention Diagnostic," Halo '03, ICFA Advanced Beam Dynamic Workshop, Montauk, NY, USA (2003).
- [5] J. R. Zagel, D. J. Harding, B. C. Brown, H. D. Glass, L. R. Koziem, S. M. Pruss, J. T. Volk, "Permanent Magnet Ion Profile Monitor at the Fermilab Main Injector." TPAH036, Proc. 2001 PAC., Chicago.
- [6] K. Wittenburg, "Experience with the Residual Gas Ionization Beam Profile Monitors at the DESY Proton Accelerators," Proc. 1992 EPAC., 24.3.-28.3, Berlin, Germany and DESY HERA 92-12
- [7] C. Fischer, "Results on Prototype Measurements for LHC Beam Instruments," Proc. 2001 DIPAC, Grenoble, France.
- [8] J. Wiza, *Microchannel Plate Detectors*, Nucl. Instr. Meth. **162** (1979) 587-601.
- [9] Laird Technologies, www.lairdtech.com
- [10] Behlke Electronic GmbH. www.behlke.de.
- [11] H. Hartmann and T. Kerner, "RHIC Beam Synchronous Trigger Module," Proc. 1999 IEEE PAC.
- [12] J. Wei, A. Fedotov, W. Fischer, N. Malitsky, G. Parzen, and J. Qiang, "Intra-beam scattering theory and RHIC experiments", ICFA Advanced Beam Dynamics Workshop on High Intensity Particle Accelerators, Bensheim, Germany, AIP Conference Proceedings (2004, to be published)
- [13] F. Pilat, et. al., "Operations and Performance of RHIC as a Cu-Cu Collider." PAC, Knoxville, TN (2005).
- [14] J. Wei, U. Iriso, M. Bai, M. Blaskiewicz, P. Cameron, R. Connolly, A. Della Penna, W. Fischer, H. Huang, R. Lee, R. Michnoff, V. Ptitsyn, T. Roser, T. Satogata, S. Tepikian, L. Wang, S.Y. Zhang, "Electron-Ion Effects at RHIC Transition", PAC, Knoxville, TN (2005)
- [15] A. Drees, "Heavy Ions in RHIC-How to get to higher Luminosities?", 21st Winter Workshop on Nuclear Dynamics, Breckenridge, CO, USA (2005).
- [16] H. Huang, et. al., "A New Relative Proton Polarimeter for RHIC," Proc. 2001 PAC, Chicago.
- [17] M. Gasior, CERN, internal email.